X-693-76-47
PREPRINT

NASA TM X- 71081

TERRESTRIAL KILOMETRIC RADIATION: 1 - SPATIAL STRUCTURE STUDIES

J. K. ALEXANDER

M. L. KAISER

MARCH 1976

GSFC

GODDARD SPACE FLIGHT CENTER

GREENBELT, MARYLAND

TERRESTRIAL KILOMETRIC RADIATION:

1 - SPATIAL STRUCTURE STUDIES

J.K. Alexander and M.L. Kaiser
Radio Astronomy Branch
Laboratory for Extraterrestrial Physics
Goddard Space Flight Center
Greenbelt, Maryland

ABSTRACT

Observations of lunar occultations of the earth at 250 kHz obtained with the Radio-Astronomy-Explorer-2 satellite have been used to derive two dimensional maps of the location of the sources of terrestrial kilometric radiation (TKR). By examining the two dimensional source distributions as a function of the observer's location (lunar orbit) with respect to the magnetosphere, we can estimate the average three dimensional location of the emission regions. Although TKR events at 250 kHz can often be observed at projected distances corresponding to the 250 kHz electron gyro or plasma level ($R \sim 2\ R_E$), many events are observed much farther from the earth ($5 \leq R \leq 15\ R_E$). On the dayside, we observed emission apparently in the region of the polar cusp and the magnetosheath at $\Lambda \sim 75^o$, and in the night hemisphere we find emission associated with regions of the magnetotail at $\Lambda \geq 70^o$. The nightside emission is suggestive of a mechanism involving plasma sheet electron precipitation in the pre-midnight sector.

TERRESTRIAL KILOMETRIC RADIATION:

1 - SPATIAL STRUCTURE STUDIES

J.K. Alexander and M.L. Kaiser
Radio Astronomy Branch
Laboratory for Extraterrestrial Physics
Goddard Space Flight Center
Greenbelt, Maryland

ABSTRACT

Observations of lunar occultations of the earth at 250 kHz obtained with the Radio-Astronomy-Explorer-2 satellite have been used to derive two dimensional maps of the location of the sources of terrestrial kilometric radiation (TKR). By examining the two dimensional source distributions as a function of the observer's location (lunar orbit) with respect to the magnetosphere, we can estimate the average three dimensional location of the emission regions. Although TKR events at 250 kHz can often be observed at projected distances corresponding to the 250 kHz electron gyro or plasma level ($R \sim 2\ R_E$), many events are observed much farther from the earth ($5 \leq R \leq 15\ R_E$). On the dayside, we observed emission apparently in the region of the polar cusp and the magnetosheath at $\Lambda \sim 75^o$, and in the night hemisphere we find emission associated with regions of the magnetotail at $\Lambda \geq 70^o$. The nightside emission is suggestive of a mechanism involving plasma sheet electron precipitation in the pre-midnight sector.

Recent satellite measurements of intense, nonthermal, kilometer-wavelength emissions from the earth can provide an important new perspective in the study of particle-field interactions in the magnetosphere. Although such emissions were observed with satellite-borne instruments more than 10 years ago, the real breakthrough in our understanding has come from recent experiments at very high altitudes which have good frequency resolution and excellent angular resolution. When the remote observations at long radio wavelengths are considered together with the results of *in situ* measurements of magnetospheric particles and fields, we may be able to provide new insight into the dynamical behavior of magnetospheric plasma.

In this paper we present an overview of the spatial structure of the terrestrial kilometric radiation (TKR). Our findings are based on two years of source position measurements obtained with the lunar-orbiting Radio-Astronomy-Explorer-2 (RAE-2) satellite. By observing the variation of the projected source positions as a function of viewing geometry throughout many lunar months, we can develop a statistical picture of the three-dimensional location of the TKR source. The emission apparently originates from a wide range of distances from the earth in regions as remote as the dayside magnetopause and the distant magnetotail, and it appears to be yet another manifestation of the transport of solar wind plasma into the ionosphere.

The first detailed spectral measurements of TKR were made by Dunckel et al. (1970) and Brown (1973) who noted that the intense, sporadic emission was concentrated in a rather narrow band which peaked between 150 and 300 kHz. Gurnett and co-workers (Gurnett, 1974; Kurth, Baumback, and Gurnett, 1975) showed that the emission was apparently an auroral phenomenon since it was observed primarily over the nighttime earth (centered at about 22 hr local time) at high latitudes and was closely correlated with the occurrence of bright auroral arcs. Further evidence for the relationship between TKR and auroral activity was provided by Gurnett (1974) who showed that TKR events were associated with magnetospheric substorms as indicated by the auroral electrojet index (AE). Kaiser and Stone (1975) noted a correlation between the TKR occurrence pattern and the patterns of auroral electron precipitation reported by Hartz (1971). Although the first time-averaged measurements of the source location by Kurth et al. (1975) and by Kaiser and Stone (1975) suggested that the emission originated from very near the earth ($R < 2\ R_E$), Kaiser and Alexander (1976) subsequently found that it was not unusual to observe the source to be situated at distances of more than 7 R_E.

We have used two-dimensional source position measurements from RAE-2 lunar occultations to investigate the TKR source locations in detail. In contrast to the earlier one-dimensional position measurements which were often averaged over 10 hr or longer, the

occultation technique provides a two-dimensional "snapshot" measurement every 3.7 hr. Our objective has been to determine whether there are recurrent patterns in the observed source locations that will permit us to identify the regions of TKR generation and to relate them to other magnetospheric phenomena. There are a number of other aspects of the TKR morphology such as the spectral variations of the emission and the evolution of TKR "storms" as a function of substorm phase to which we shall allude. However we will defer a detailed discussion of those facets of the problem for subsequent papers in this series.

We will begin by describing those technical aspects of the investigation that are important in understanding the data including an illustration of the occultation technique, a definition of the data selection criteria, and a discussion of experimental errors. We then describe the apparent beaming pattern of the TKR in the ecliptic plane since an appreciation of this aspect of the emission is important both in interpreting the RAE-2 position data and in developing a theory for the origin of TKR. The major findings of this study are then presented in a series of projections of source locations as a function of viewing geometry. After illustrating the more detailed source behavior by describing several specific events of particular interest, we conclude with a discussion of the apparent three-dimensional source geometry and its relation to major features of the magnetosphere.

One semantic note is in order before beginning. After Gurnett (1974) introduced the term "terrestrial kilometric radiation" (TKR), Kurth et al. (1975) presented strong arguments that would favor the more specific name "auroral kilometric radiation". As the results of our study will show, however, it is still not completely clear that all the observed emissions are strictly auroral. Therefore, we have preferred to continue the use of the more general "TKR" to identify the emission.

MEASUREMENT TECHNIQUE

Instrumentation

In July 1973, the RAE-2 spacecraft was placed in a circular lunar orbit with an altitude of 1100 km, an inclination to the Moon's equator of 60°, and a period of 222 min. Since the RAE-2 instrumentation has been described in detail elsewhere (Alexander et al., 1975) we will only summarize those aspects of the experimental system essential to the occultation analysis. We have used data from the long V-antenna that is pointed downward toward the Moon. At kilometric wavelengths, sources near the Moon's limb will always be included in the main lobe of the antenna pattern. The 32-channel burst receiver on the lower V-antenna covers a frequency range of 25 kHz to 13.1 MHz and obtains one sample at each frequency every 8 sec. For typical occultation events, this sample rate corresponds to approximately 8 samples per R_E of motion of the projection of the Moon's limb on the plane

through the earth perpendicular to the earth-Moon line. The usable dynamic range for receiver frequency channels in the TKR spectral range is greater than or equal to 40 dB. Wideband signals in excess of about 50 dB above background begin to cause nonlinear effects in the wideband pre-amplifiers at the receiver front-end. Although this introduces problems in obtaining good spectral data for intense events, it does not seriously affect occultation timing measurements in the center of the TKR band.

Occultation geometry

As viewed from RAE-2, the Moon has an angular diameter of 76° and the earth has a diameter of 2°. Lunar occultations of the earth occur for a period of about 7 days every other week. The geometry of the lunar occultations is illustrated in Figure 1. For three different occasions in November 1973, we have shown the projection of the Moon's limb at 2-min intervals on the plane through the earth perpendicular to the earth-Moon line. Also shown are the orientation of the earth's magnetic dipole axis and the terminator separating the day and night hemispheres of the earth as viewed from RAE-2. The occultation geometry varies from a grazing event on Nov. 1 to a central occultation on Nov. 5. The optimum period for determining source positions from occultations is typified by the intermediate case on Nov. 2. Here the angular motion of the Moon's limb across the earth has a rate of approximately 1 R_E/min and there is no ambiguity concerning the location of the point of intersection of the limb projections at the times of disappearance

and reappearance of the terrestrial radio source. Central occultations, on the other hand, provide more nearly one-dimensional position estimates, are ambiguous, and are subject to position uncertainties due to any timing errors. Consequently, we have used only those events that satisfied the geometrical advantages illustrated by the Nov. 2 example. During each 7-day occultation series approximately 30 such optimal events occur so there are about 750 occultations per year that could be used.

Our approach has been to examine the radio data for each usable occultation period and to estimate the two-dimensional boundaries of the source based on the following four times:

1) t_1 = time at which emission first begins to decrease at first contact of Moon's limb with the source,
2) t_2 = time at which emission has fallen to 10% of its value at t_1,
3) t_3 = time at which emission has risen to 10% of its value at t_4, and
4) t_4 = time at which emission completely returns to its pre-occultation level at last contact of Moon's limb with the source.

The intersections of the limb positions at these four times should bound the region from which 90% of the radiation originates.

This procedure is illustrated in Figure 2 for an occultation observed on August 25-26, 1974. This event is noteworthy because there is evidence for three different components to the radio

emission resulting in three distinct intensity levels or steps in the occultation curve. The four occultation contact times, t_1 - t_4, are indicated by the dashed lines in the lower panel of the Figure for each of the three sources which we have labelled A,B, and C. The resultant source positions are shown in the upper-portion of the Figure 2. Since the Moon was near first quarter phase, RAE-2 was situated approximately over the dusk side of the earth and the source positions are projections on the noon-midnight meridian plane. Note that all three sources are associated with the nighttime hemisphere, and the weaker components (B and C) appear to be situated in the magnetotail at projected distances of 3 and 5 R_E, respectively. All of the sources have characteristic dimensions of approximately 1 R_E.

Selection effects

Examination of TKR events observed with the IMP-6 satellite by R.G. Stone and J.R. Herman (private communication) shows that the frequency of peak TKR flux is most often between 250 and 300 kHz. The RAE-2 data indicate that the peak in TKR occurrence probability also occurs in the 250-300 kHz band. Therefore, we have concentrated on measurements at 250 kHz in the present study.

A number of selection criteria were used to determine what occultation events were to be included in the study. As we have already noted, central occultation events were not used since they yield ambiguous results. Also, we discarded all events that could have been affected by simultaneous signals from solar radio bursts

or from receiver intermodulation effects at 250 kHz due to intense signals received outside the TKR frequency range. No TKR events with observed intensity levels less than 10 dB above the cosmic noise background were used. Particularly bursty events, for which an unambiguous estimate of the disappearance and reappearance times could not be made, were also discarded. Perhaps the most important selection criterion in the present study was the requirement that the flux levels of the TKR be essentially the same (within ~ 5 dB) at ingress and egress. We have no a priori evidence to suggest that the location of a source changes as its intensity changes, and an earlier less restrictive analysis of the RAE-2 data gave results that were not substantially different from those to be presented here. Nevertheless, we have preferred to apply the requirement of approximately constant source intensity during the occultation period in order to reduce any ambiguity related to possible source evolution during the measurement. About half of all observed TKR occultations satisfied these selection criteria. This editing process, combined with the effects of an average RAE-2 duty cycle of ~ 70% and an average TKR occurrence rate of ~ 50%, resulted in a total of 260 TKR occultations which were used in this study.

Measurement uncertainty

There are three classes of error or uncertainty which must be considered in interpreting the RAE-2 occultation position measurements.

These are (1) experimental measurement errors, (2) propagation effects and (3) uncertainties due to assumptions implicit in the selection process. Of these, only the experimental measurement errors can be easily estimated and quantified. We often observe signals (both man-made and thunderstorm) which originate near the surface of the earth at frequencies above the ionospheric critical frequency (~ 3 MHz). From measurements of their projected source locations on the disk of the earth we can regularly confirm that any spacecraft timing or ephemeris errors correspond to positional uncertainties of less than 1 R_E. In most cases, the TKR source dissappearance and reappearance times can be estimated to less than 1 min uncertainty which also corresponds to a projected positional error of less than 1 R_E with respect to the center of the earth.

All source location data presented in this study are apparent positions as determined by the observed occultation times without any attempt to apply corrections for refraction effects. If the emission is generated at or near the local electron plasma or gyro frequency at auroral latitudes, then for 250 kHz radiation the source would be located at a radial distance of the order of 2 R_E. Those ray paths that intercept the Moon could pass through a portion of the outer plasmasphere at high latitudes. We would expect any refraction in the plasmasphere to move the apparent position equatorward to a projected position closer to the center of the earth, and we will

present evidence later that this effect may sometimes occur. For sources that are situated at large distances from the earth (e.g. $R > 4\ R_E$) we would not expect any significant plasmaspheric refraction unless the source is at equatorial latitudes and over the opposite hemisphere of the earth from the Moon. Plasma densities in the outer magnetosphere and the interplanetary medium are too low to cause significant refraction at 250 kHz. Measurable changes in apparent source positions would also be expected if there was a substantial lunar ionosphere; however, there is no systematic evidence in our data to suggest that this effect occurs.

In addition to refraction, the TKR waves may experience scattering by irregularities in the medium along the ray path from the source to RAE-2. Vesecky and Frankel (1975) made a lower limit calculation of scattering by density fluctuations in the earth's magnetosheath and estimated that the scattered source size would be less than 1° at 200 kHz. We find source sizes at 250 kHz of typically 1 R_E or 1° which is not inconsistent with that estimate. The effect of scattering will be to change the apparent source size but not its position. We will defer a more detailed analysis of those effects for a later paper.

To obtain an estimate of a source position from occultation data we must assume that the source is stationary during the interval

between its disappearance and reappearance. There is evidence both in the RAE-2 data and in the findings of Kurth et al. (1975) that significant source motion can sometimes occur in periods of less than an hour. Consequently, we recognize that care is necessary in interpreting individual isolated events. Our requirement that the source flux level be essentially unchanged at the beginning and end of an occultation is intended to reduce the effect of possible source motion by concentrating on events that are relatively stable over the course of the measurement. The repeatability in source location patterns that we observe over many months of data suggests that our statistical results are not being grossly distorted by source motion effects.

OBSERVATIONS

TKR radiation pattern

A very important aspect of TKR morphology is the apparent radiation pattern as inferred from variations in the average intensity level and in occurrence probability as a function of the observer's location with respect to the earth. Gurnett (1974) showed that the IMP-6 spacecraft observed TKR most often over the evening sector of the earth. He found a pronounced maximum in the 178 kHz occurrence probability distribution between 22 and 24 hr magnetic local time (MLT) and a minimum of activity in the 6 to 12 hr MLT sector. Kaiser and Stone (1975) used observations at 130 kHz

from RAE-2 to show that events exceeding a level of 20 dB above cosmic noise were most often observed over the 20 to 24 hr MLT sector and were practically non-existent over the 4 to 16 hr MLT hemisphere.

The RAE-2 findings at 250 kHz based on all data from July 1973 through June 1975 are shown in Figure 3. We display the percentage occurrence probability of emission at intensities greater than 10 and 30 dB above cosmic noise background and also the average power flux observed at 250 kHz as a function of the local time on the earth at the sub-lunar point. (Observations corresponding to approximately 12 hr local time are obtained at new Moon, 18 hr at first Quarter, 24 hr at full Moon, and 06 hr at last Quarter.) Each 1-hr. local time bin represents the results of 475 hr $\pm$ 37 hr (1σ) of observations corresponding to 2.2×10^5 individual samples. The behavior of the TKR source over this two-year period represents an average over a $\pm$ 35° range of magnetic latitude at the sub-lunar point. The TKR occurrence and power statistics show a broad region of enhanced activity between 16 and 04 hr local time with a peak in the 21-22 hr bin. There is a sharp minimum in the distribution at 9 hr local time.

The apparent TKR "radiation pattern" illustrated in Figure 3 presumably results from a combination of the intrinsic radiation pattern of the source and subsequent propagation effects between the source and the observer outside the magnetosphere. Some aspects of this problem have been discussed by Gurnett (1974) and Benson (1975), and further investigation of the TKR beaming pattern should provide insight into the nature of the emission

mechanism. The apparent beaming pattern also plays a role in determining the local time distribution of TKR events available for study in our present analysis of source positions. As a consequence of the relative minimum in the activity profile in the morning sector there are approximately half as many occultation measurements per local time interval between 5 and 15 hr as in the remaining range of viewing angles in our survey. The largest number of events which contributed to our position studies fell in the 16 to 18 hr local time range when RAE-2 was situated nearly over the dusk meridian of the earth.

Average source position projections

Since the derived two-dimensional source locations are projections on a plane perpendicular to the earth-Moon line, we have grouped the results according to the lunar phase at the time of the measurement to sort out variations due to viewing geometry. We have then superimposed all source positions derived for a particular lunar phase to examine the statistical variation of projected source positions as a function of orientation of the magnetosphere with respect to the observer.

The choice of the most appropriate co-ordinate system for displaying the TKR position data is not immediately obvious. The nature of that problem is illustrated in Figure 4 where we have super-imposed all source positions obtained when the sub-lunar magnetic local time (MLT) was between 15 and 18 hr for three

different co-ordinate systems. In each case the X'-Z plane is approximately the 1030-2230 MLT meridian plane and the +X' direction is sunward. In Figure 4a we have used the geocentric solar magnetospheric system in which the X' axis is parallel to the ecliptic plane and the +Z direction is in the northern ecliptic hemisphere. In Figure 4b we have used the geocentric solar magnetic system so that the Z axis is parallel to the geomagnetic dipole with North positive. In Figure 4c, the Z axis is also parallel to the geomagnetic dipole, but the +Z direction always includes that geomagnetic pole that is tilted towards the Sun (i.e. the daytime pole). Consequently, in Figure 4c the North pole is more often in the +Z direction in April through September and the South pole is generally in the +Z direction in October through March. In all three systems we can see the tendency for TKR to be observed more often over the nighttime hemisphere, but there is considerable spread in the source locations when the data are displayed using the two conventional co-ordinate systems (Figure 4a and b). The source position distribution is more tightly organized in Figure 4c where we take the tilt of the dipole with respect to the Sun into account. Most of the sources that are located over the daytime hemisphere are associated with the daytime pole (Z positive) and the probability of observing emission over the night hemisphere is highest above nighttime polar regions (Z negative). Since the data do seem to be better organized when the sense of the dipole

tilt with respect to the Sun is considered, we will use the system illustrated in Figure 4c in all the displays that follow.

The distribution of TKR source positions as a function of viewing geometry is shown in Figure 5. For each 3-hr sub-lunar MLT interval we have displayed the frequency of occurrence of TKR at a given position with respect to the earth by dividing the projection plane into 1-R_E grid elements. In each plot the sunlit portion of the earth visible from RAE-2 is to the left and the Z axis is parallel to the dipole axis with the daytime pole toward the top.

Beginning in Figure 5 with the 12-15 hr MLT interval, we see that most of the emission observed from this viewpoint is projected on the evening hemisphere with a higher occurrence probability associated with the magnetic hemisphere tilted away from the Sun (Z negative). The low probability of TKR at projected distances less than 1 R_E may be partially due to obscuration by the plasmasphere as was suggested by Gurnett (1974). The results for the 15-18 hr MLT zone have already been discussed in reference to Figure 4c. From this perspective, the TKR distribution is characterized by a narrow daytime feature and a broad evening population. The concentration of sources observed over the nighttime equatorial region at about 2-3 R_E may be due, in part, to refraction in the dusk plasmasphere between the sources (at higher latitudes) and the observer (in the ecliptic plane). Notice also that no significant emission from distances greater than 3 R_E is observed

from the lower left-hand quadrant. The character of the distribution is different in the 18-21 hr MLT sector where the emission is observed in each quadrant of the diagram. This changing character of the distribution continues into the region of peak TKR activity in the 21-24 hr MLT sector. Here we see two "horns" of emission in the positive Z hemisphere, a maximum projected over the nighttime pole at about 1-2 R_E, and a tilted feature running from large radial distances on the dusk side of the -Z hemisphere to nearer the equator on the dawn side of the -Z hemisphere.

The TKR source distribution is more compact over the 00-03 hr MLT sector and again has a peak in occurrence probability at a projected location over the nighttime magnetic pole ($1 \leq |Z| < 2\ R_E$). The observations from the 03-06 hr MLT interval closely resemble the observations from the zone 180^o away at 15-18 hr. No significant emission is observed from the upper right-hand quadrant and the tendency for evening sources to favor the nighttime pole is particularly notable. Over the 06-09 hr MLT sector the general level of TKR activity is quite low, and the number of available source position measurements is too small to show any significant pattern in the source distribution. In the 09-12 hr MLT sector we find most sources tend to be situated close to the earth ($R \leq 5\ R_E$).

To obtain some perspective of the positions of TKR sources in terms of the major features of the magnetosphere, we have

projected the centers of those sources observed at times near quarter phase of the Moon onto a noon-midnight meridian plane plot of the MF73D magnetic field model (Mead and Fairfield, 1975) in Figure 6. We have excluded observations at times when the dipole was tilted significantly out of the projection plane ($\geq 20^{o}$) and we have made a small "projection correction" by rotating the positions from an assumed location in the projection plane of the measurement to the noon-midnight meridian plane. Most of the sources centered on the dayside of the earth at $R > 5\ R_E$ are at magnetic latitudes near the polar cusp, and the most distant of those sources are located near the region of the bow shock above the dayside cusp. On the nightside, those sources in the +Z hemisphere appear to trace out the 70^{o} field line whereas the sources in the -Z hemisphere are apparently associated with field lines between 70^{o} and 80^{o} in the geomagnetic tail. At distances inside about 4 R_E there is appreciable scatter in the projected source centers. Although some of the scatter is most certainly due to dynamic variability in the real positions of TKR sources, a part of this effect is also probably due to projection effects, plasmaspheric refraction, and our basic measurement uncertainty ($\pm$ 1 R_E rms). In spite of those complications, we can see from Figure 6 there is a strong tendency for the TKR sources to be associated with field lines that map to high latitudes near the auroral zones.

Specific examples

Before discussing the implications of the TKR position distributions in more detail, we will present several examples of individual measurements which illustrate the source behavior in the major regions of activity. These events are not necessarily "typical" cases in every sense, but they have been selected to emphasize certain features of the average position distribution which appear to be important in understanding the origin of the radiation and its relevance to magnetospheric dynamics.

Figure 7 shows two examples of observations obtained from over the late afternoon sector which show sources projected near the poleward edge of the plasma sheet in the magnetotail. In Figure 7a we see the results from three consecutive lunar occultations on April 27, 1974, when the sub-lunar MLT was approximately 16 hr. In all three cases we observe multiple sources with the most intense component close to the earth and the more distant (and weaker) source components situated at $R \geq 6\ R_E$ above the nighttime pole at 70-75° magnetic latitude. For the third occultation (at about 0935 UT) when the emission had increased in both intensity and bandwidth, we find the primary source to occupy a large area over the nighttime portion of the Northern hemisphere. In Figure 7b, we show four consective observations from February 18, 1975, when RAE-2 was nearly in the dusk meridian plane (sub-lunar

MLT ~ 17.5 hr.). Only the first occultation at about 0915 UT yields a single source close to the earth. In the three subsequent measurements we find multiple sources with projected positions between 2 and 9 R_E above the southern magnetic hemisphere at geomagnetic latitudes between 65° and 75°.

In Figure 8, we have two examples of occultation positions obtained nearer the time of full moon when RAE-2 was located over the nighttime hemisphere in the region of maximum TKR activity. Figure 8a shows the positions derived from three consecutive orbits on March 7, 1974 when the sub-lunar MLT was 23.3 hr. For the first two events we find a projected position at $R \simeq 2.7\ R_E$ above the Northern hemisphere on the dusk side of the midnight meridian. The third occultation, which occurred after the emission intensity had increased considerably, results in multiple components along a line that passes through the vicinity of the first two sources out to a maximum distance of nearly 9 R_E. The orientation and alignment of the projected source positions is consistent with what one might observe if the emission came from along high-latitude field lines corresponding to a slightly earlier local time than that at the observer's location.

In Figure 8b we see five consecutive measurements obtained on April 3 and 4, 1974, when the sub-lunar MLT was about 22 hr. Except for the event at 0700 UT, all sources project to locations more

directly above the North magnetic pole than in the March 7 example at distances between about 3 and 5 R_E. Both the series of measurements illustrated in Figure 8 and the distant group of sources shown in Figure 7a are suggestive of emission from a region threaded by magnetic field lines at about 75° magnetic latitude above the nighttime pole in the 21 to 22 hr MLT zone.

A final set of individual position measurements is shown in Figure 9. The source at 1935 UT on November 6, 1973, when the sub-lunar MLT was 20.4 hr has at least four components. The most intense ($\succ$ 40 dB above background) component was apparently located above the Northern auroral region at $R \simeq 10\ R_E$. In addition, we observe weaker (10-30 dB above background) emission from multiple locations at high latitudes on the dayside at distances ranging from 4 to 15 R_E. It is noteworthy that these observations correspond to a period of magnetospheric substorm activity. The north-south component of the interplanetary magnetic field had been significantly southward for the order of 1 hr before the measurement ($B_Z \sim -2.5\ \gamma$) and the auroral electroject index (AE) was greater than 400γ during the period. The observation on November 16, 1973, was obtained from above the dawn meridian at a sub-lunar MLT of 5.5 hr. Again we find multiple source components above the dayside hemisphere at distances of 7 to 14 R_E. This event occurred during a period of moderate substorm activity (AE $\succeq$ 200 γ). For both dates, the dayside sources are associated with the dayside magnetic pole

(Z positive) at projected positions near the dayside polar cusp at 75° to 80° latitude. The outermost source components at $R \succ 10\ R_E$ would appear to be located in the region where the cusp opens into the magnetosheath.

DISCUSSION

The general picture of the average TKR source locations that emerges from these measurements can be roughly divided into two components - nightside and dayside. TKR is more often observed over the night hemisphere in a region centered in the pre-midnight sector near 22 hr local time. Nighttime sources observed at large distances from the earth ($\succ 4\ R_E$), where measurement uncertainties and possible plasmaspheric refraction effects are not critical, are concentrated near magnetotail field lines at 70° to 80° geomagnetic latitude. On the dayside, emission is observed less often so that we cannot determine any preferred local time location, but we find that nearly all sources observed at $R \succ 4\ R_E$ are projected near the latitude of the polar cusp above the <u>daytime</u> pole.

In addition to those aspects of the source distributions which we have described in detail above, there are certain trends in the data which have been analyzed in a more cursory fashion and which lend further support to the concept of TKR emission from along a narrow range of magnetospheric field lines at a given instant. When multiple source components are observed in an occultation, we

usually find all components to be arranged along a line as would be the case if they were all confined to a particular flux tube or sheet. In such multiple sources, the most intense component is almost always closest to the earth and the weakest component is the most distant. This brightness distribution would be expected from a radiation mechanism in which the emission intensity depends directly on the source particle density and/or magnetic field. Our preliminary investigation of the variation of source locations with observing frequency indicates that the source distance also varies directly with wavelength so that emission at higher frequencies ($\gtrsim$ 300 kHz) is usually observed to come from closer to the earth than emission at lower frequencies ($\lesssim$ 250 kHz). These multiple frequency source locations also can be "fit" on a field line in many cases.

A preliminary analysis of the 1973 data indicates most of our TKR events are associated with auroral disturbances as indicated by high values of AE ($\gtrsim$ 150), but the correlation is certainly not perfect. Examination of the association of dayside emission with substorm phenomena yields a similar result. At least 75% of the 1973 sources that have projected positions over the daytime hemisphere correspond to times when AE was greater than 200 and the north-south component of the interplanetary magnetic field was southward.

The RAE-2 data are consistent with the suggestion by Gurnett (1974) that TKR is associated with inverted-V electron precipitation events. In the late evening and midnight sectors the inverted-V bands have been observed by Frank and Ackerson (1972) near the poleward

edge of the plasma sheet, and Craven and Frank (1975) have reported similar precipitation events in the dayside polar cusp. The circumstantial evidence for association of TKR with electron precipitation is strengthened further by a number of other observations that imply that the region of frequent TKR activity near 22 hr local time is a region of special importance in magnetospheric substorm morphology. For example, Lesniak and Winkler (1970) used electron measurements at synchronous altitudes to deduce a "fault line" in this region that divided areas of geomagnetic inflation (westward) and collapse (eastward) during substorms; Hoffman and Burch (1973) found that the patterns of nightside electron precipitation were more organized with respect to substorm phase in the premidnight sector; and McDiarmid et al. (1975) proposed that entry and energization of magnetosheath particles into the magnetosphere was greater in the premidnight sector due to field line reconnection occurring in this region.

The premidnight sector is also important as the location of the region of reversal of convection electric fields in the auroral ionosphere - i.e. the Harang discontinuity (Maynard, 1974). Convective flow patterns change from being predominantly westward to predominantly eastward around 22 hr MLT at the poleward edge of the auroral zone and just before 24 hr MLT at the equatorward edge of the auroral zone.

Although we have emphasized those regions of the TKR position distributions where the probability of occurrence is highest, it

is important that one not overlook the dynamic complexity of the emission. We have already noted that evidence for a change in source location between consecutive RAE-2 orbits (3.7 hr) is not unusual, and that we sometimes have evidence for source motion during a single occultation (~ 40 min). At small distances from the Earth ($R < 4\ R_E$) there is considerable scatter in the occultation positions, and some emission has been observed at all latitudes over both the day and night hemispheres. Some of this scatter is undoubtedly a result of projection effects, measurement errors and propagation effects. At the present time, however, we cannot rule out the possibility that there are occassions when TKR is generated close to the earth at sub-auroral latitudes. Further detailed analyses are required in order to resolve this question and to provide a clearer picture of the extent of the emission in latitude and local time.

As we noted at the beginning, this survey has concentrated on developing an overview of the source position morphology at a single frequency near the center of the TKR spectral band. Future work must certainly include a study of the detailed frequency dependence of source location and observations of the spatial and spectral evolution of TKR events and their correlation with substorms. The additional perspective provided by those investigations should help us begin to understand the emission mechanism and the relationship of TKR to magnetospheric dynamics.

Acknowledgement: The authors express thanks to Ms. P. Harper and S. Vaughan for their assistance with data processing.

REFERENCES

Alexander, J.K., M.L. Kaiser, J.C. Novaco, F.R. Grena, and R.R. Weber, Scientific instrumentation of the Radio-Astronomy-Explorer-2 satellite, Astron. & Astrophys. 40, 365, 1975.

Benson, R.F., Source mechanism for terrestrial kilometric radiation, Geophys. Res. Lett., 2, 52, 1975.

Brown, L.W., The galactic radio spectrum between 130 and 2600 kHz, Astrophys. J., 180, 359, 1973.

Craven, J.D. and L.A. Frank, Electron angular distributions above the dayside auroral oval, Univ. of Iowa rept. 75-23, 1975.

Dunckel, N., B.Ficklin, L. Rorden, and R.A. Helliwell, Low-Frequency noise observed in the distant magnetosphere with OGO 1, J. Geophys. Res., 75, 1854-1862, 1970.

Frank, L.A. and K.L. Ackerson, Local-time survey of plasma at low altitudes over the auroral zones, J. Geophys. Res., 77, 4116, 1972.

Gurnett, D.A., The earth as a radio source: Terrestrial kilometric radiation, J. Geophys. Res., 79, 4227, 1974.

Hartz, T.R., Particle Precipitation Patterns, The Radiating Atmosphere, p. 225, B.M. McCormac, Ed., Reidel, Dordrecht, Netherlands, 1971.

Hoffman, R.A., and J.L. Burch, Electron precipitation patterns and substorm morphology, J. Geophys. Res., 78, 2867, 1973.

Kaiser, M.L. and R.G. Stone, Earth as an intense planetary radio source: Similarities to Jupiter and Saturn, Science, 189, 285, 1975.

Kaiser, M.L. and J.K. Alexander, Source location measurements of terrestrial kilometric radiation obtained from lunar orbit, Geophys. Res. Lett., 3, 37, 1976.

Kurth, W.S., M.M. Baumback and D.A. Gurnett, Direction-finding measurements of auroral kilometric radiation, J. Geophys. Res., 80, 2764, 1975.

Lezniak, T.W. and J.R. Winkler, Experimental Study of magnetospheric motions and acceleration of energetic electrons, J. Geophys. Res., 75, 7075, 1970.

Maynard, N.C., Electric Field measurements across the Harang Discontinuity, J. Geophys. Res., 77, 4620, 1974.

McDiarmid, I.B., J.R. Burrows and E.E. Budzinski, Average characteristics of magnetospheric electrons (150 eV to 200 eV) at 1400 km, J. Geophys. Res., 80, 73, 1975.

Mead, G.D. and D.H. Fairfield, Quantitative magnetospheric models derived from spacecraft magnetometer data, J. Geophys. Res., 80, 523, 1975.

Vesecky, J.F. and M.S. Frankel, Observations of a low-frequency cutoff in magnetospheric radio noise received on IMP-6 J. Geophys. Res., 80, 2771, 1975.

FIGURE CAPTIONS

Figure 1 - Variations in RAE-2 lunar occultation geometry. The arcs are projections of the Moon's limb at 2-min intervals (labelled in HHMM format) on the plane through the earth perpindicular to the line-of-sight. The orientation of the earth's magnetic dipole axis and the day and night hemispheres are shown as seen from RAE-2.

Figure 2 - An example of an occultation of TKR observed by RAE-2 at 250 kHz. The multiple steps during the occultation indicate three source regions. The four "contact" times of each step (lower panel) define the source regions as shown in the upper panel.

Figure 3 - The power and occurrence probability patterns of TKR at 250 kHz as a function of local time. The heavily-shaded inner histogram is the relative power pattern. The lightly-shaded outer histogram is the percentage occurrence of noise greater than 10 times the galactic background. The middle histogram is the percentage occurrence of noise greater than 1000 times the background. All three plots show a peak in the 21-22 hr time bin.

Figure 4 - Source location occurrence distributions displayed in three different coordinate systems. The top panel is the Geocentric Solar Magnetosphere (GSM) ystem (as viewed from 15-18 hr) where +Z is in the northern ecliptic hemisphere and the abscissa is parallel to the ecliptic plane with the sun toward the left. The middle panel is the Geocentric Solar Magnetic (SM) System with the Z axis along the geomagnetic dipole (+Z toward north). The system used in the bottom panel is similar to the SM system except that +Z is always the geomagnetic pole tilted sunward.

Figure 5 - Accumulated source positions as viewed from different local times. The coordinate system is the same as the bottom panel of Figure 4 with +Z along the daytime geomagnetic pole. The abscissa rotates by 3 hr from panel to panel, but the sun is always toward the left. The shading indicates the relative emission occurrence probability as a function of location on a 1 R_E grid.

Figure 6 - Source centers viewed from over the dawn and dusk terminators projected onto the noon-midnight meridian plane (with +Z the sunlit geomagnetic pole). The overlay is selected field lines from the Mead-Fairfield (1975) magnetic field model MF73D.

Figure 7 - Two series of occultations viewed from near first-quarter Moon. The MLT at the sub-lunar point is given along with the date and approximate UT of each observation. The coordinate system is that used in Figure 4c overlayed with selected field lines from the Mead-Fairfield (1975) magnetic field model MF73D. Both the April 27 series from three successive orbits and the February 18 series from four successive orbits suggest emission along the poleward edge of the plasma sheet in the magnetotail.

Figure 8 - Two series of occultations viewed from full Moon. The format is the same as Figure 7. The orientation and alignment of the projected source positions suggests emission from along high-latitude field lines originating at a slightly earlier local time than that at the observer's location.

Figure 9 - Source positions along the dayside cusp. The format is the same as Figure 7.

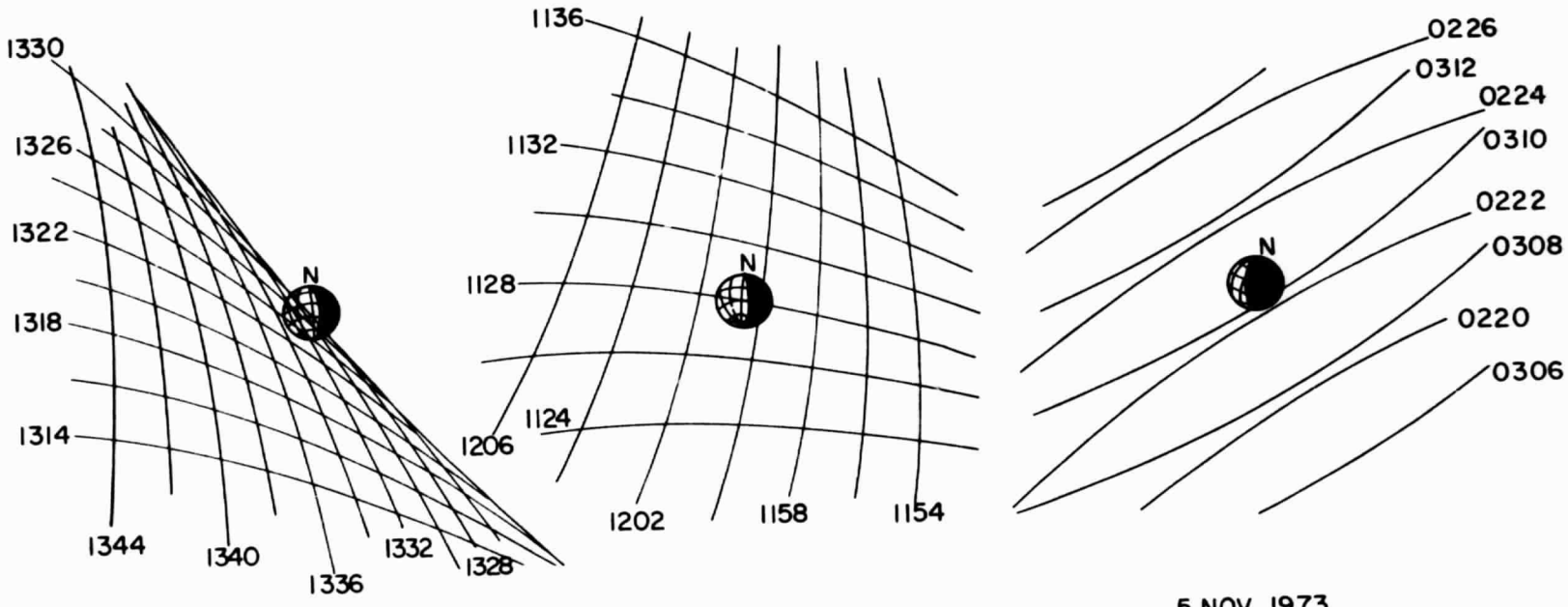

1 NOV. 1973

2 NOV. 1973

5 NOV. 1973

Figure 1

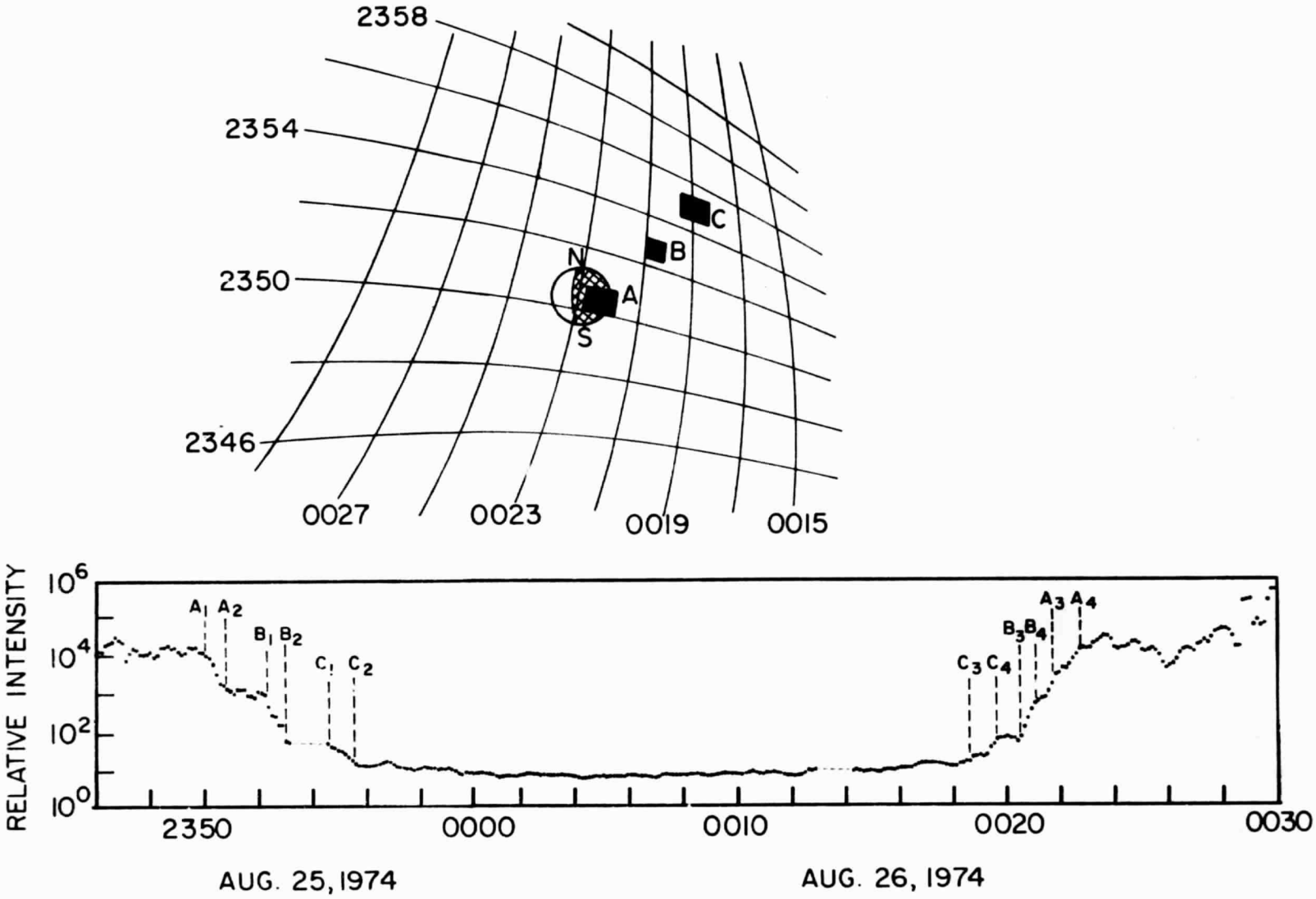
2358
2354
2350
2346
0027
0023
0019
0015
N
S
A
B
C
RELATIVE INTENSITY
10^6
10^4
10^2
10^0
A_1 A_2
B_1 B_2
C_1 C_2
C_3 C_4
B_3 B_4
A_3 A_4
2350
0000
0010
0020
0030
AUG. 25, 1974
AUG. 26, 1974

Figure 2

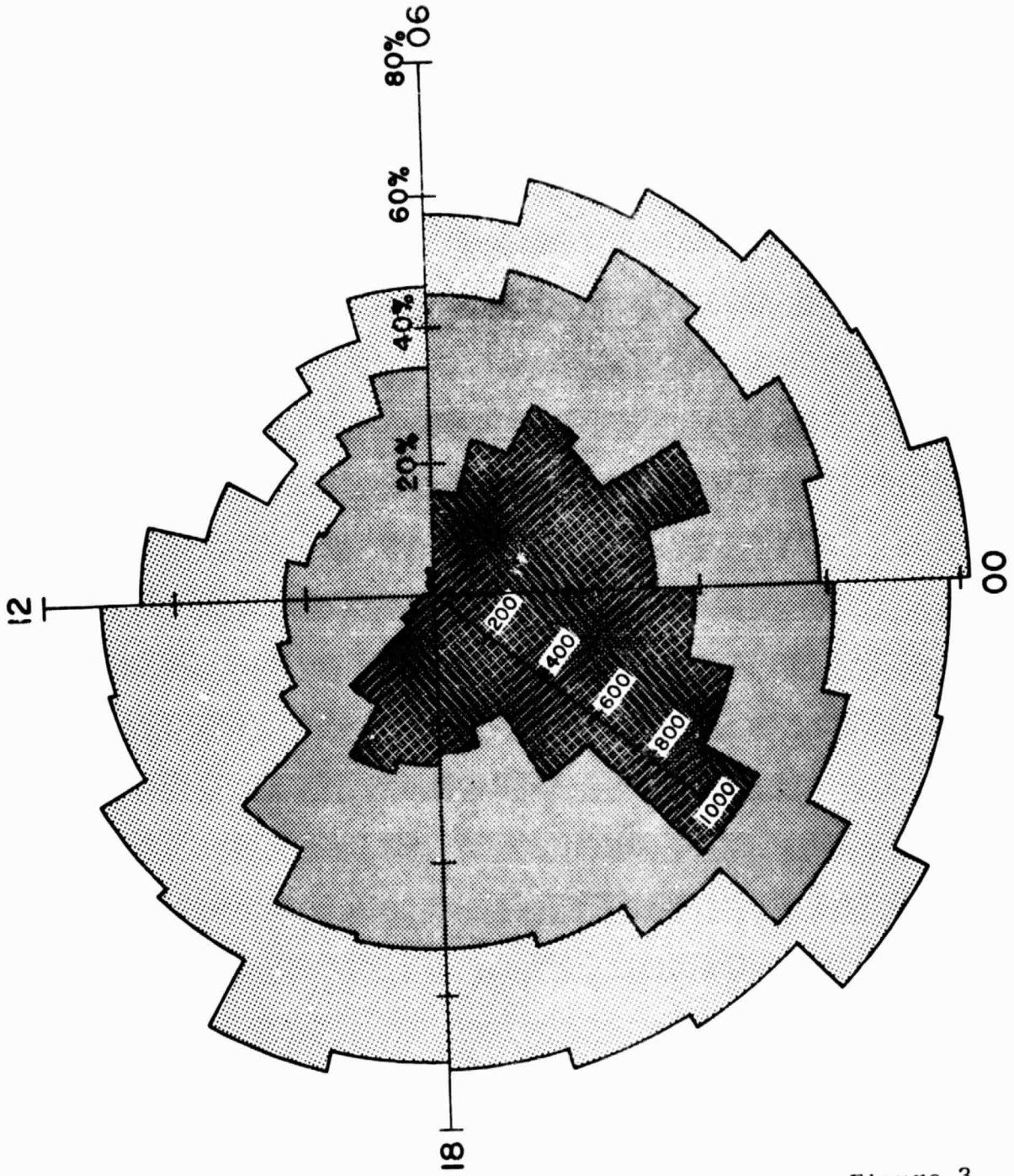

Figure 3

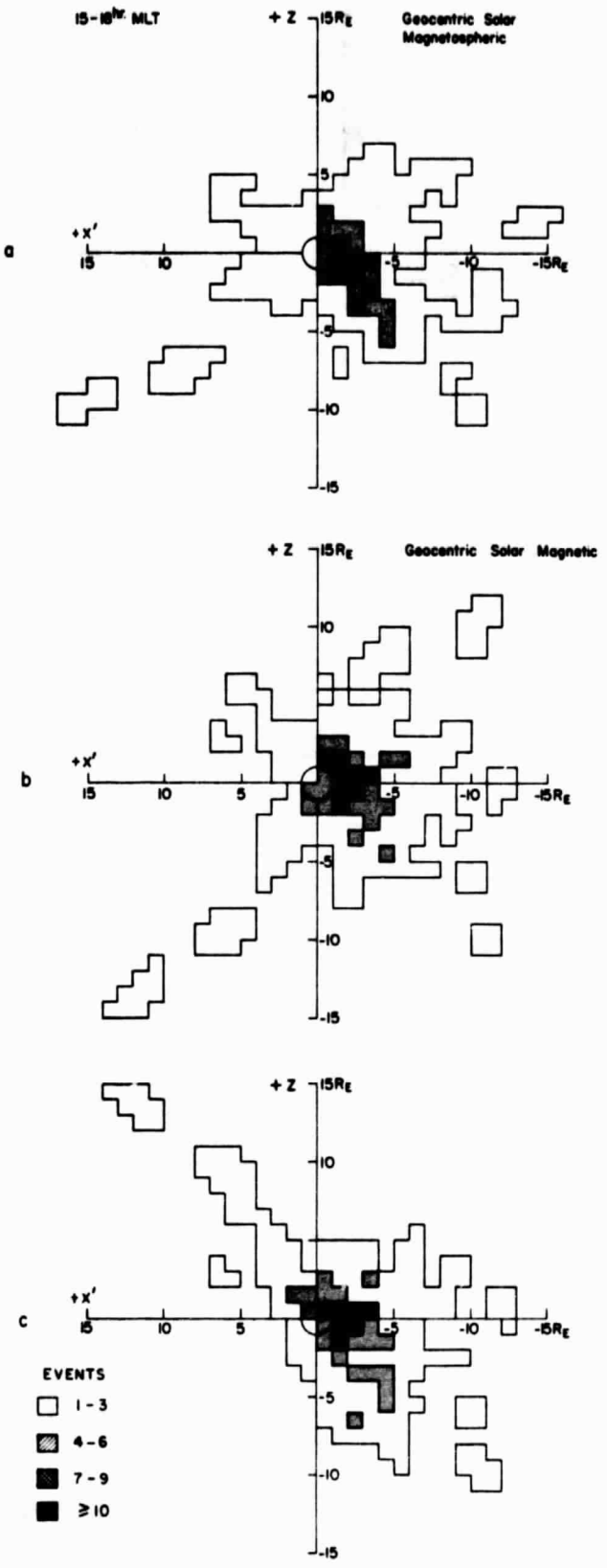
15 - 18hr. MLT
+ Z
15RE
Geocentric Solar Magnetospheric
10
5
+X'
15
10
-5
-10
-15RE
-5
-10
-15
a
+ Z
15RE
Geocentric Solar Magnetic
10
+X'
15
10
5
-5
-10
-15RE
-5
-10
-15
b
+ Z
15RE
10
+X'
15
10
5
-5
-10
-15RE
-5
-10
-15
c
EVENTS
1 - 3
4 - 6
7 - 9
≥ 10

Figure 4

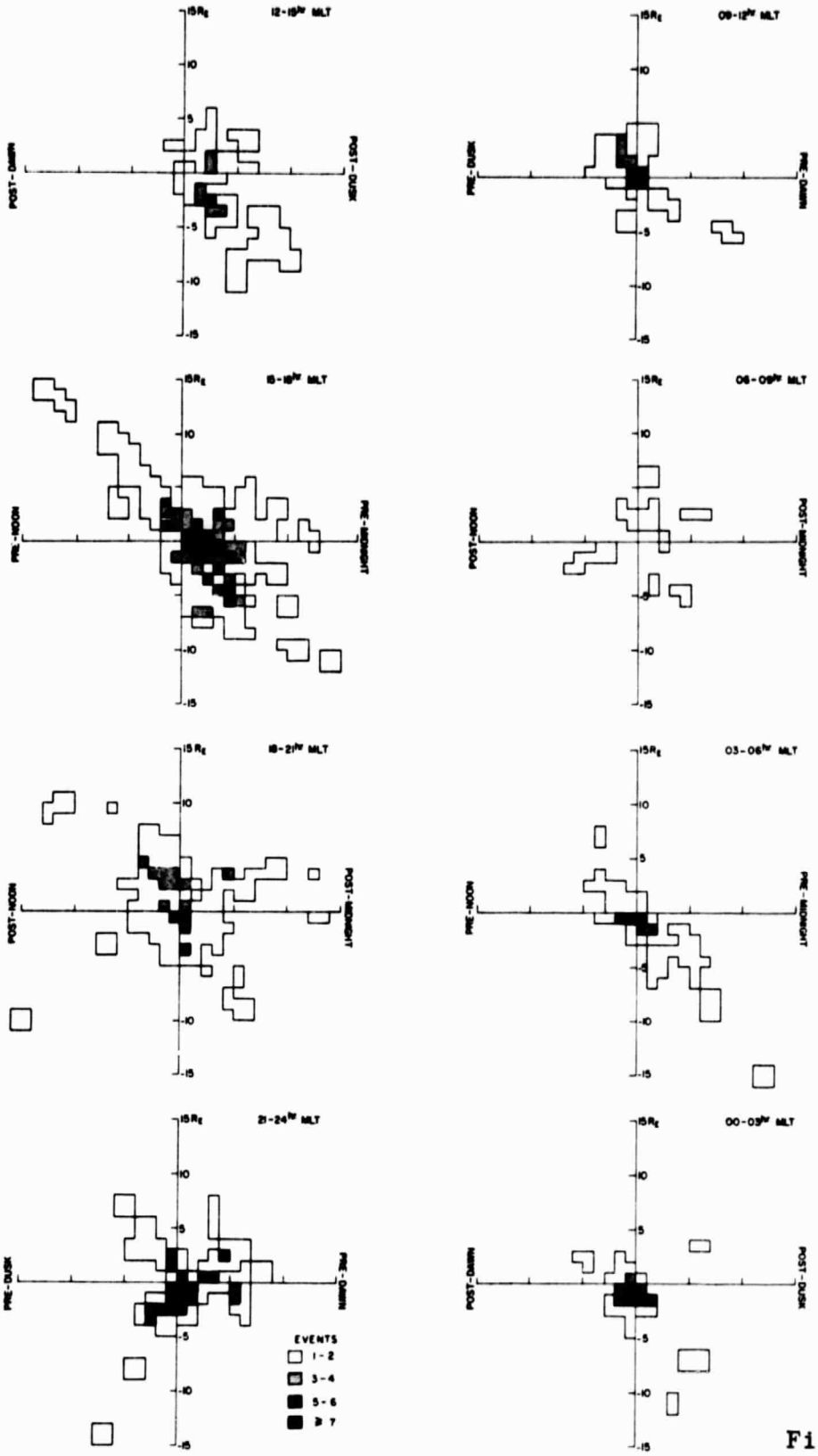
12-15 HR MLT
09-12 HR MLT
15-18 HR MLT
06-09 HR MLT
18-21 HR MLT
03-06 HR MLT
21-24 HR MLT
00-03 HR MLT
POST-DAWN
POST-DUSK
PRE-DUSK
PRE-DAWN
PRE-NOON
PRE-MIDNIGHT
POST-NOON
POST-MIDNIGHT
EVENTS
1-2
3-4
5-6
≥ 7

Figure 5

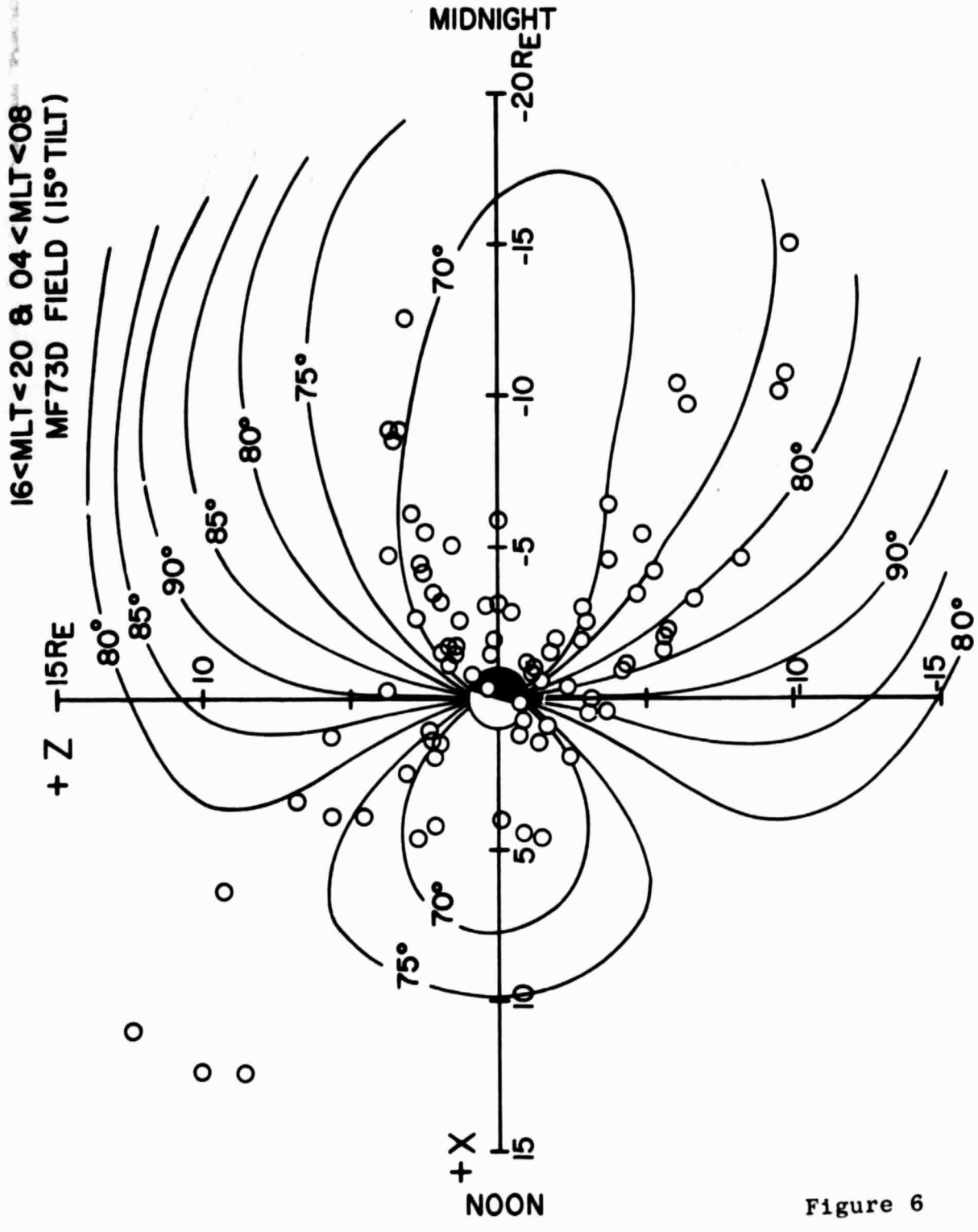
16<MLT<20 & 04<MLT<08
MF73D FIELD (15° TILT)
MIDNIGHT
-20RE
-15
-10
-5
70°
75°
80°
85°
90°
15RE
10
+Z
5
10
15
+X
NOON

Figure 6

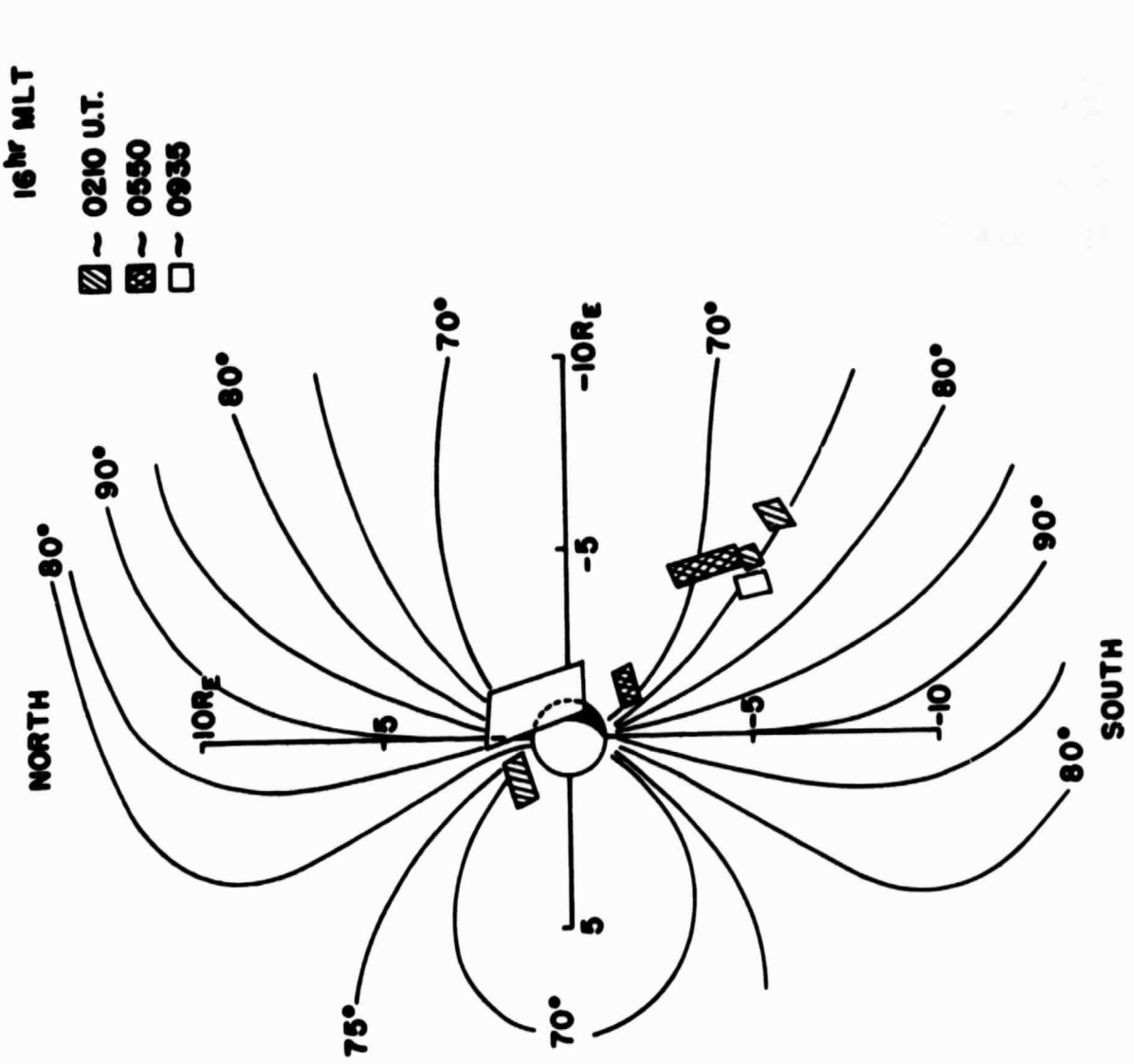
27 APR. 1974
16^hr MLT
~ 0210 U.T.
~ 0550
~ 0935
NORTH
SOUTH
80°
90°
80°
70°
-10R_E
70°
80°
90°
80°
10R_E
5
-5
-5
-10
5
75°
70°

Figure 7a

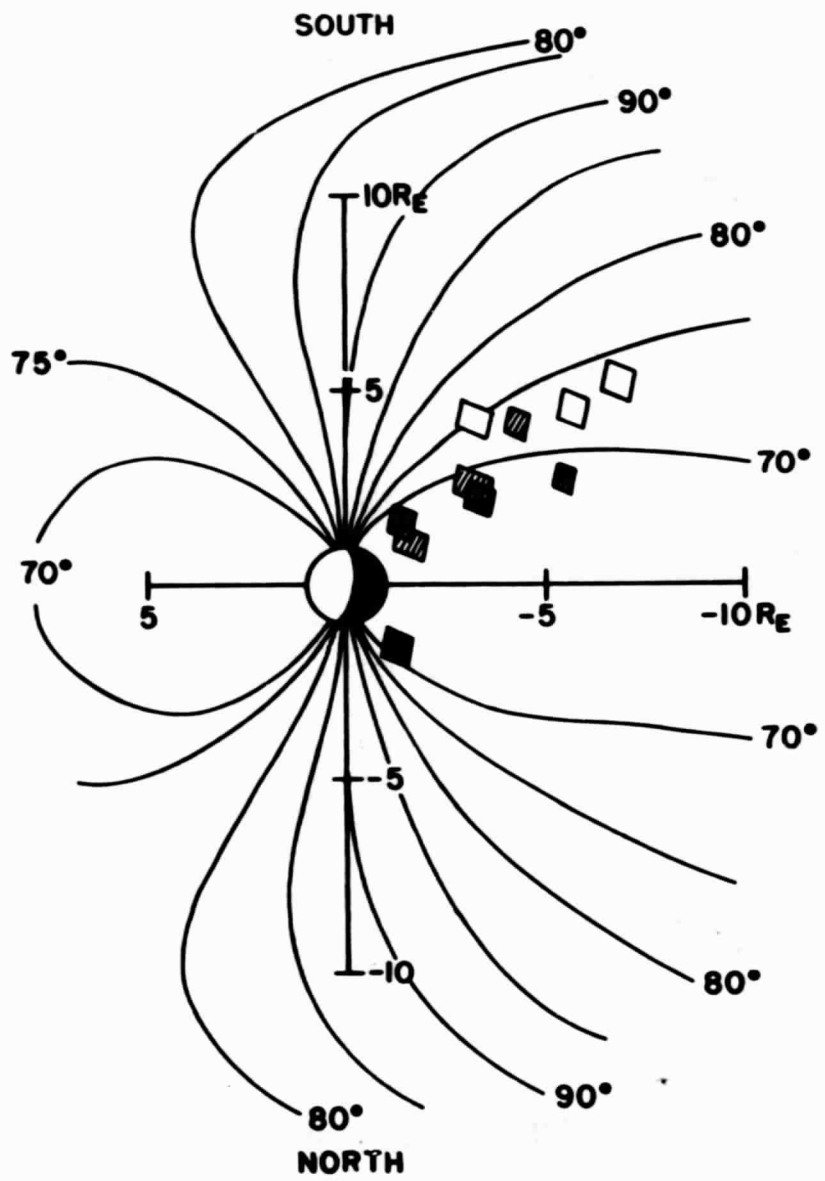
SOUTH
80°
90°
10RE
80°
75°
5
70°
70°
5
-5
-10RE
70°
-5
-10
80°
90°
80°
NORTH
18 FEB. 1975
17.5 MLT
~ 0915 U.T.
~ 1255
~ 1635
~ 2020

Figure 7b

APR 3-4, 1974
21.8 MLT
1 - 2338 U.T.
2 - 0315
3 - 0700
4 - 1040
5 - 1425
PRE-DAWN
-5R_E
SOUTH
5R_E
-5
-10
NORTH
5
PRE-DUSK
MAR. 7, 1974
23.3 MLT
1 - 0935 U.T.
2 - 1315
3 - 1655
DAWN
-5R_E
SOUTH
5R_E
-5
-10
NORTH
5
DUSK

Figure 8

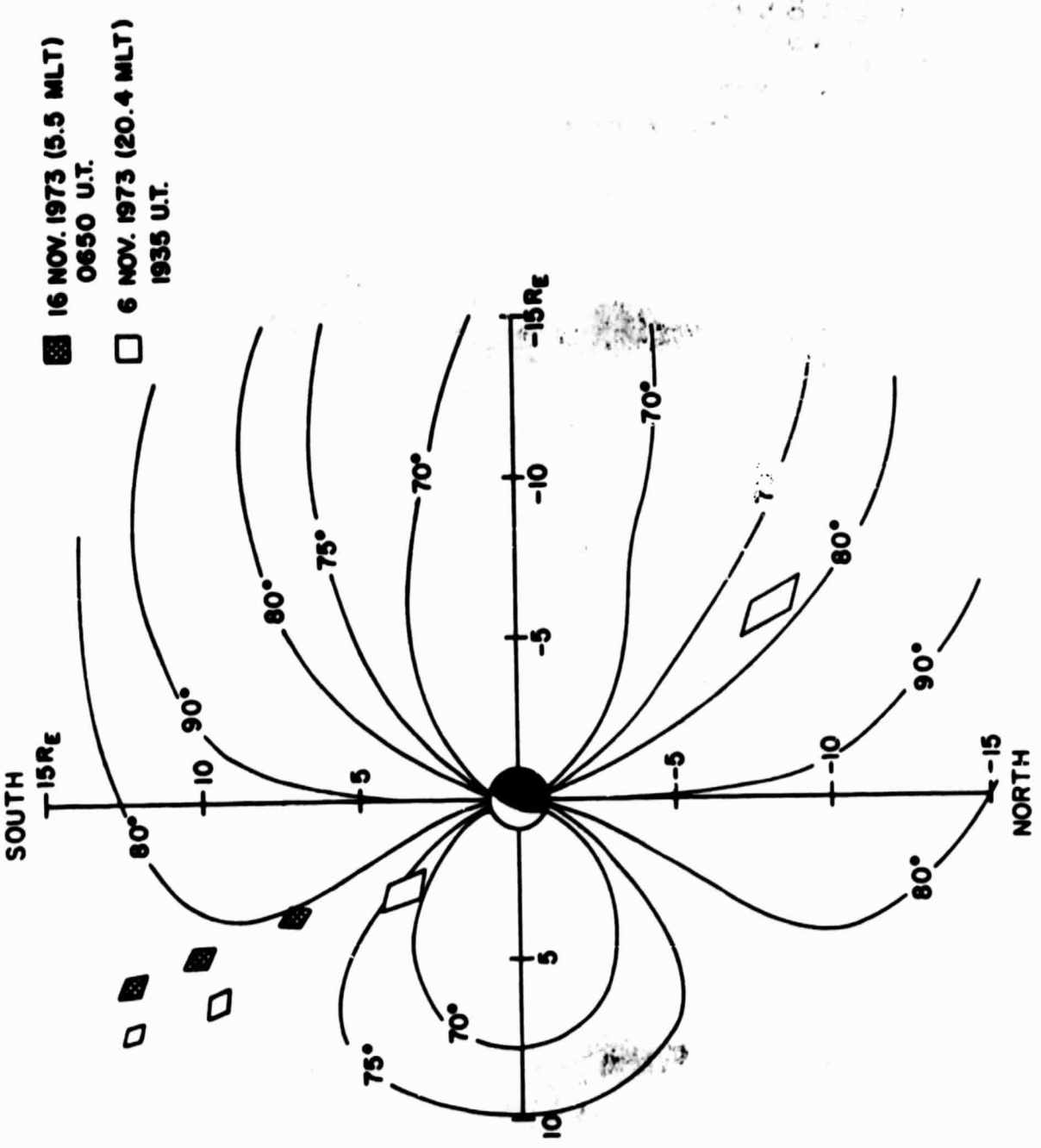
16 NOV. 1973 (5.5 MLT)
0650 U.T.
6 NOV. 1973 (20.4 MLT)
1935 U.T.
SOUTH
15R_E
NORTH
-15R_E
90°
80°
75°
70°
10
5
-5
-10
-15

Figure 9